

# Resistance Spot Welding of Complex Stack-Ups using Electric Servo-Guns

Jerry Gould, Menachem Kimchi  
*Edison Welding Institute*

## Abstract

In this program, the capabilities of medium-frequency direct current (MFDC) electric servo resistance welding guns for the welding of complex stack-ups were investigated. Capabilities of interest from these guns include the ability to apply forge forces and currents, as well as the ability to sequence the current and forging profiles. The complex stack-up under study included a 1-mm outside sheet attached to two 2-mm sheets. Work was done using design-of-experiment (DOE) techniques. The experiment included a range of processing variations deliverable from the MFDC servo-gun, as well as two electrode variations (materials and sizes). Heat balance during resistance welding this stack-up was found to be dominated by the electrode variations. As electrode variations are not considered a solution for automotive complex stack-up applications, a best practice was defined from the DOE that included similar-sized Class 2 electrodes. This best practice included short overall weld times, a moderate forge force, a significant (40%) increase in current during forging, and a weld time relative to the forging portion of the weld schedule. This yielded nugget penetrations of roughly 50% into the thin attached sheet. It was noted that at these penetrations, indentations on both sides of the joint reached 0.45-mm, and that process variations could be used to trade off penetrations with overall indentations.

## Introduction

The automotive body-in-white has seen some of the more dramatic changes in the last two to three model generations than in any other equivalent period in its history [1,2,3]. These changes are a result of two-fold pressure being applied by the needs to improve fuel economy and body rigidity. Each of these factors also has multiple sub-influences. The uncertain supply of crude oil, increased demand for gasoline (both in developing as well as industrialized countries), and more stringent government regulations to combat pollution are some of the primary factors pushing automotive original equipment manufacturers (OEMs) to develop ever more efficient vehicles. The government is also having a marked impact on the drive for body rigidity to accommodate more challenging crash testing. The consumer demand for better handling and a more firm "feel" when driving also pushes OEM designers toward stiffer body structures.

The need for increased fuel efficiency and improved body rigidity are usually counterproductive to one another. If a body-in-white design had only to consider fuel efficiency, the gauges of the steels could simply be reduced to lighten the weight. Contrarily, if the needs were only to address crash worthiness/rigidity issues, this could be accomplished by increases in the steel gauges of the structure. The balance between these issues was helped with the introduction of high-strength and advanced high-strength steels (HSS, AHSS) [2,3]. A traditional B-Pillar frame member may have been composed of 2.5-mm-thick 270 MPa steel. With use of HSS material, a designer could both improve crash-worthiness and reduce weight by selecting 2.0-mm-thick DP 600 material.

This improvement, naturally, does not come without penalty. The costs, weldability, and formability of these higher strength materials add new challenges to manufacturing. One of these challenges is the welding of complex stack-ups. Complex stack-ups are typically defined as multiple sheets (more than two) with varying gauges. The most challenging of these for resistance welding are those attempting to attach a thin outer sheet to

a stack-up of thicker materials. For automotive applications, this can include a thin sheet, nominally 0.6- to 0.8-mm, attached to a metal combination that can be up to 5- to 6-mm thick.

Resistance welding of such stack-ups becomes a heat balance problem. This heat balance problem becomes manifest through reduced penetration in the thinnest outside sheet in the stack-up. This problem has been addressed thoroughly in available reference literature for resistance welding [4,5]. Standard solutions have included the use of different-sized, as well as different-composition, electrodes to improve heat balance. These approaches essentially use electrodes with different heat-conducting capability to promote nugget formation in a way to allow attachment of the thinnest sheet. While such approaches have proven successful for many decades [4,5], they are not suitable for current automotive manufacturing. This is reflected in current recommended starting resistance welding practices [6] suggesting a single-sized electrode for stack-ups up to several millimeters. For these applications, there are concerns with the cost implications of maintaining several different-sized/material electrodes for the various stack-ups that can occur on a vehicle. In addition, the availability of electrodes with varying sizes/materials increases the possibility that mistakes can be made, potentially exacerbating the heat balance problems with these candidate stack-ups.

Achieving heat balance for complex stack-ups using similar-sized electrodes has also been evaluated using numerical modeling techniques [7]. This particular work addressed heat balance when the electrode face size was relatively small compared to the total complex stack-up thickness. In that work, it was found that relatively small electrodes could effectively draw the developing fusion zone close to the electrodes, attaching the thin outside sheet. However, in this case, excessive melting occurred at the outside sheet/middle sheet contact surface, resulting in aggressive expulsion. This study recommended not using small electrode sizes to attach such thin outside sheets on these stack-ups.

A more pragmatic approach to achieving proper heat balance in complex stack-ups has been studied by applying the “law of thermal similarities”[8,9]. The law of thermal similarities is essentially a one-dimensional thermal analysis of spot weld stack-ups, predicting new processing schedules based on geometric ratios (based on thickness). The approach has been applied directly [8] and while incorporating both latent heats and dimensional changes (indentation) during welding [9]. While these approaches offer insights into welding practices for different total stack-up thicknesses; however, they do not offer insights into attachments of a thin outer sheet onto these stack-ups.

An alternative approach is to look at applications of forge forces to improve attachment of the outside sheet in a complex stack-up. Forge forces (force increases at or near the end of the current pulse) have commonly been used to improve joint quality on both aluminum and nickel-based alloys [5]. However, systems capable of applying force forces are not commonly applied for automotive applications. This has changed recently with the introduction of electric servo-guns [10, 11, 12]. Electric servo-guns apply welding forces through the use of an electric motor and a mechanical actuation device (typically a ball-screw). Welding force, then, can be directly controlled by the current supplied to the motor itself. The systems originally offered advantages of extended opening displacements, and rapid force rises (shorter squeeze times). However, the close relationship between motor current and force allows forge cycles to be used in automotive applications. The use of such force forces has recently been demonstrated for improvements in resistance weld quality for aluminum sheet [13].

In this program, the ability of the servo-gun to accomplish forge forces as well as the coordination between forces and currents has been used to improve the weldability of complex stack-ups. Weldability, in this case, was defined as the ability to attach the thin outside sheet during the operation. To better characterize the relationships between weld gun parameters and final joint quality, DOE techniques were used [14, 15, 16]. In this way, quantitative inferences could be drawn between various gun factors and a range of measures of final weld quality.

## Experimental Approach

Complex stack-ups for resistance welding in an automotive context can potentially cover a wide range of joint configurations. To reduce the vagueness implicit in the term, discussions were held with a range of automotive OEMs and Tier 1 suppliers [17, 18, 19, 20, 21]. The answers received varied. Some manufacturers discussed developing a better understanding of welding transformation-induced plasticity (TRIP) and twinning-induced plasticity (TWIP) materials. Others talked about welding non-ferrous materials, single-sided spot welding, and welding through adhesives. One constant discussed by each manufacturer, however, was the so-called thin/thick weld stack. These types of weld stacks are seen throughout the body-in-white wherever two thick frames are welded to an accompanying floor panel or skin side panel. Through these discussions, it was noted that the specifics of the stacks varied from manufacturer to manufacturer. In general, most manufacturers are currently limited to DP 600 in their existing production manufacturing processes and do not have immediate plans for increasing beyond this strength level. Gauges range from 1.4-mm to over 2.0-mm. The thin sheet materials being used were generally on the order of 250-300 MPa with a thickness range 0.65- to 0.75-mm. After comparing the data gathered, it was determined that the most representative weld stack for study was a three high stack with a configuration 2.0-mm DP 590 to 2.0-mm DP 590 to 0.7-mm 270, with each sheet having a galvaneal coating.

Work in this program was done on an MFDC integral transformer electric servo C-frame welding gun. This unit is controlled by a proprietary ARO iBox control unit. This unit is fully integrated and allows easy program access and flexibility for program modification. In addition, the ARO control unit also has pre-determined outputs for data acquisition. Actual data acquisition in this study was handled in two ways. First, all welds were monitored with a Miyachi 326B weld monitor. This was primarily done for a quick examination of root mean square (rms) weld currents. More detailed monitoring was done both through the ARO iBox interface (as noted above) and with external instrumentation. Weld current and force signals were taken directly from the ARO unit. The displacement was measured using a linear potentiometer. All data collection was done with a Yokogawa DL750 digital storage oscilloscope.

To examine relationships between both the processing variables described above, as well as different electrode configurations, DOE techniques were employed. The specific experiment selected was an 8-factor, 2-level, 32-run 2 [3, 4, 5, 6, 7, 8] fractional-factorial design. This DOE is a Resolution IV design, in which eight of the possible 28 2-factor interactions are confounded. The variables in this experiment included, as follows:

- Preliminary electrode force
- Ratio of the secondary to preliminary electrode force
- Total weld time
- Fraction of the weld time used for primary current flow
- Number of pulses during secondary current flow
- Ratio of secondary to primary current level
- The material used for the electrode contacting the thin sheet in the stack-up
- Ratio of the thick- to thin-side electrode diameters

The first six of these factors are directly reduced from the allowed process variables discussed above. The last two relate to variations in electrode configuration. Specifically, Resistance Welder Manufacturers Association (RWMA) Class 2 and RWMA Class 3 copper electrodes were used, and machined to 6.4- and 8-mm face

diameters as appropriate. The Stage 1 current was set proportionally to Stage 1 weld time using the standard joule heating equation for resistance spot welding (RSW), shown in Eq. (1):

$$H = I^2 R t \quad (1)$$

where  $H$  is the heat generated in the weld,  $I$  is the applied welding current,  $R$  is the total resistance of the weld, and  $t$  is the effective current on time. For Stage 2 pulsation schedules, the cool time was 30 ms. Actual levels for these various factors were based on some preliminary experiments.

As mentioned above, the actual experimental design used in this study had eight 2-factor interactions confounded with other 2-factor interactions. To practically use this experiment it was necessary to identify six of these potential 2-factor interactions that could be eliminated from consideration. The selection of these six 2-factor interactions was done using prior experience with RSW processes. This was done by first assessing the potential significance of each candidate 2-factor interaction based on this experience. The six ranked lowest in potential significance were then assumed negligible for the purposes of this experiment.

The actual confounding arrangement is characteristic for the specific design of experiment used. The actual confounded interactions then are based on assignment of individual experimental input variables to specific columns in the experimental design. For the experimental design used here, column assignments were made to assure that the six lowest-ranked interactions were only confounded with those of higher assessed significance. This essentially allowed the 20 top-ranked interactions to be included in the subsequent analysis confounded (at worst) only with the six lowest-ranked ones. The resulting confounding scheme is presented in Table 1.

Table 1 Matrix of Confounded Interactions for the DOE used in this Study

<b>Dominant Interaction</b>	<b>Secondary Interaction(s)</b>
Top electrode material × electrode diameter ratio	Weld time × Stage 1-2 WT timing, W2 pulsation × force Stage 1
Top electrode material × weld time	Electrode diameter ratio × Stage 1-2 WT timing
Top electrode material × W2 pulsation	Electrode diameter ratio × force Stage 1
Top electrode material × force ratio 2-1	none
Electrode diameter ratio × Weld time	Top electrode material × Stage 1-2 WT timing
Electrode diameter ratio × W2 pulsation	Top electrode material × force Stage 1
Top electrode material × I level 2-1	None
Electrode diameter ratio × force ratio 2-1	None
Electrode diameter ratio × I level 2-1	None
Stage 1-2 WT timing × force Stage 1	Weld time × W2 pulsation
Weld time × force ratio 2-1	None
Weld time × force Stage 1	W2 pulsation × Stage 1-2 WT timing
Weld time × I level 2-1	None
W2 pulsation × force ratio 2-1	None
W2 pulsation × I level 2-1	None
Force ratio 2-1 × Stage 1-2 WT timing	None
Force ratio 2-1 × force Stage 1	None
Force ratio 2-1 × I level 2-1	None
Stage 1-2 WT timing × I level 2-1	None
Force Stage 1 × I level 2-1	None

The resulting experimental design associated with the confounding scheme of Table 1 is provided in Table 2. This experimental matrix has been converted into machine programmable factors. This includes specific values of electrode materials/sizes, as well as each process parameter of interest.

Table 2 DOE Matrix Converted into Actual Machine Programmable Factors

Trial No.	Thin Sheet Side Electrode Configuration		Preliminary Force and Current			Secondary Force and Current			
	Material (Class)	Face Diameter (mm)	Force (N)	Weld Time (ms)	Weld Current (kA)	Force (N)	No. Pulses	Pulse Width (ms)	Weld Current (kA)
1	2	6.4	2400	110	10.0	1600	2	85	12.0
2	2	6.4	1700	270	8.0	1890	1	150	11.2
3	2	6.4	2400	270	8.0	2670	2	75	9.6
4	2	6.4	1700	110	10.0	1130	1	170	14.0
5	2	6.4	1700	270	8.0	1130	1	150	9.6
6	2	6.4	1700	110	10.0	1890	1	170	12.0
7	2	6.4	2400	270	8.0	1600	2	75	11.2
8	2	6.4	2400	110	10.0	2670	2	85	14.0
9	2	8	1700	170	9.3	1130	2	125	11.2
10	2	8	2400	170	9.3	2670	1	250	11.2
11	2	8	2400	170	9.3	1600	1	250	13.1
12	2	8	1700	180	9.1	1130	2	50	12.7
13	2	8	2400	180	9.1	1600	1	100	10.9
14	2	8	1700	180	9.1	1890	2	50	10.9
15	2	8	1700	170	9.3	1890	2	125	13.1
16	2	8	2400	180	9.1	2670	1	100	12.7
17	3	6.4	2400	170	9.3	2670	1	250	13.1
18	3	6.4	2400	180	9.1	2670	1	100	10.9
19	3	6.4	1700	180	9.1	1130	2	50	10.9
20	3	6.4	2400	180	9.1	1600	1	100	12.7
21	3	6.4	1700	170	9.3	1130	2	125	13.1
22	3	6.4	1700	170	9.3	1890	2	125	11.2
23	3	6.4	2400	170	9.3	1600	1	250	11.2
24	3	6.4	1700	180	9.1	1890	2	50	12.7
25	3	8	1700	110	10.0	1890	1	170	14.0
26	3	8	2400	270	8.0	2670	2	75	11.2
27	3	8	2400	270	8.0	1600	2	73	9.6
28	3	8	1700	110	10.0	1130	1	170	12.0
29	3	8	1700	270	8.0	1130	1	150	11.2
30	3	8	1700	270	8.0	1890	1	150	9.6
31	3	8	2400	110	10.0	2670	2	85	12.0
32	3	8	2400	110	10.0	1600	2	85	14.0

Seven welds were produced for each run of the experiment. These welds were used for tensile testing (three samples), chisel testing (three samples, results not included in this paper), and metallographic evaluations (one sample). 31- × 127-mm coupon size was used in the production of all test samples. Tensile testing was done in the tensile-shear configuration. Specimen geometry and test methods matched the AWS/SAR D8.9M Recommended Practice [22].

For each sample tested, electrode indentation measurements were first made at the top and bottom surfaces (the latter not included in this paper). For tracking purposes, the weld interface between the thin (top sheet) and thick middle sheet was designated as the 1-2 interface, while that between the two thick sheets (middle and lower sheet) was designated as the 2-3 interface. The peak tensile load was measured at both the 1-2 and 2-3 interfaces (the latter again not included in this paper). Button sizes were measured at each after all destructive test.

Metallographic inspections were done using standard techniques. This included sectioning along the weld centerline, grinding, polishing, and etching in a solution of saturated Picric acid in water. This etchant has been shown to successfully reveal the extents of weld nuggets in steel resistance spot welds [23]. All welds were examined using optical microscopy. Resulting micrographs were used to assess weld nugget penetration at the 1-2 interfaces.

Four measures of weld performance are then reported here as response variables. These measures were derived from the mechanical testing and metallurgical evaluations described above, and include:

- Tensile-shear strength at the 1-2 interface
- Button size at the 1-2 interface (taken from the tensile-shear and chisel test samples)
- Indentation at the outside thin sheet
- Nugget penetration into the outside thin sheet

Analysis of these results was done using standard EWI techniques [14, 15, 16]. These techniques include normalization of the response data, regression curve fitting, and presentation in robustness plots. Normalization is done through various mathematical transforms improving normality of the dataset. These transforms are 1:1 maps of the original data into a normalized space. This approach results in datasets that are best matched for statistical analysis, and produces more accurate curve fits for interpretation. Actual curve fitting is done using standard regression techniques. Of note, once curve fitting is complete, the resulting equation must be back-transformed using the inverse function associated with any normalization treatment as described above. Process robustness plots are graphical tools used to interpret the developed regression curves. These plots are essentially a series of one-dimensional sections through the multi-dimensional process spaces defined by the curves. Here, the curves themselves are first used to provide an optimized set of conditions (based on the available data). Then, through the curve-fitting equation, the factors of interest are varied one at a time over the range studied. The result is a series of profiles showing the characteristic degradation of the process associated with each factor as it is varied from its best-practice condition. Such robustness plots can be used to both identify critical processing factors, as well as set limits on allowed variations for any future manufacturing application.

## Results

The experimental results from the DOE trials are presented in Table 3. This includes three replicates of the shear load to failure at the 1-2 interface, seven replicates of the indentation measurements for the thin attached sheet, six replicates of the 1-2 interface nugget size, and one measurement of weld nugget penetration into the thin sheet. Tensile-shear data at the 1-2 interfaces (thin sheet attachment) showed only a small variation over the experiment, from nominally 4 to 6 kN. These results were reasonably consistent over the three replicates taken. Here, loads to failure were seen to vary by usually less than 10% and never more than 20%.

Table 3 Indentation Measurements for each Run of the DOE

Run	Shear Failure Load at the 1-2 Interface (kN)			Thin Sheet Side Indentation (mm)							1-2 Interface Button Size (mm)						Penn. (%)
	Rep. 1	Rep. 2	Rep. 3	Rep. 1	Rep. 2	Rep. 3	Rep. 4	Rep. 5	Rep. 6	Rep. 7	Rep. 1	Rep. 2	Rep. 3	Rep. 4	Rep. 5	Rep. 6	
1	4.7	4.5	4.8	--	--	--	--	--	--	--	6.5	7.3	7.5	7.2	6.7	6.5	40
2	4.8	4.5	4.5	0.53	0.81	0.51	0.48	0.64	0.51	0.36	6.1	6.8	5.8	7.4	7.2	7.6	0
3	4.4	4.1	4.4	0.36	0.41	0.46	0.33	0.33	0.51	0.28	6.4	4.7	6.4	3.5	5.4	4.1	7
4	5	5	5.1	--	--	--	--	--	--	--	8	8	8	7.1	7.3	6.9	47
5	3.9	4.1	4	0.25	0.25	0.3	0.23	0.28	0.25	0.25	6.3	6.3	5.7	5.5	4.9	5	6
6	4.4	4.5	4.7	0.38	0.38	0.38	0.25	0.3	0.3	0.38	6.4	6.9	7.4	5.4	5.4	6.1	33
7	4.3	4.4	4.2	0.25	0.23	0.38	0.43	0.23	0.41	0.36	6.4	5.1	6.2	5.5	4.7	5.5	0
8	4.9	5.2	5.2	0.56	0.74	0.89	0.66	0.89	0.79	0.3	7.5	8	8.3	6.7	7.7	7.2	25
9	5.1	4.9	4.9	0.66	0.41	0.41	0.43	0.48	0.38	0.48	7.7	7.7	7.5	6.2	6.3	6.5	7
10	5	4.8	5.1	0.64	1.04	0.61	0.84	0.76	0.66	0.51	8.2	7.8	8.3	6.8	7.1	6.9	33
11	5.1	5.5	5.2	0.81	0.69	0.66	1.02	0.56	0.69	1.5	8.2	8.2	8.3	6.8	7.8	7.5	31
12	4.4	4.5	4.7	0.43	0.36	0.38	0.28	0.43	0.38	0.51	7	6.8	7.1	5.7	6.2	6.5	25
13	5.2	4.6	4.5	0.38	0.36	0.51	0.43	0.71	0.51	0.69	7.2	7.3	7	6.3	6.7	6.7	50
14	4.6	4.6	4.5	0.33	0.36	0.38	0.43	0.28	0.48	0.48	6.8	6.3	6.8	5.2	6.4	6.2	40
15	5	5.9	5.2	0.69	0.46	0.64	0.71	1.17	0.56	0.66	7.7	7.8	7.7	7.4	8.6	6.2	44
16	4.9	4.8	4.8	0.99	1.35	0.86	0.71	0.81	1.02	0.99	7.9	7.8	7.9	7.5	7.1	7.5	50
17	5	4.8	5.2	1.27	1.65	1.22	1.02	1.65	0.76	0.76	7.9	8.2	9.4	7.5	7.3	7.5	38
18	4.8	4.6	4.5	0.36	0.58	0.25	0.69	0.33	0.56	0.56	7.2	7	6.5	6.7	6.9	6.6	50
19	4.5	4.4	4.4	0.3	0.33	0.3	0.3	0.33	0.33	0.33	7.1	6.7	6.6	5.8	6	5.9	60
20	4.9	4.7	4.8	0.51	0.48	0.43	0.48	0.46	0.51	0.56	7.6	7.6	7.8	6.8	7	6.9	73
21	4.9	5	5.2	0.64	0.64	0.66	0.69	0.53	0.58	0.58	8	6.6	8	7.6	7.6	7.5	67
22	4.8	4.5	4.9	0.51	0.46	0.56	0.48	0.74	0.61	0.56	7.9	7.5	7.7	6.2	6.1	6.6	73
23	5.2	5.2	5.1	0.43	0.56	0.56	0.51	0.46	0.66	0.61	8	7.3	8.1	6.3	6.4	6.5	44
24	4.4	4.4	4.2	0.36	0.33	0.38	0.38	0.36	0.36	0.36	7	7	6.9	5.3	6.2	5.8	53
25	5.2	5.2	5.1	0.71	0.61	1.04	0.43	0.56	0.74	0.58	8.8	8.1	8.7	7.5	7.6	7.7	53
26	4.4	4.5	4.4	0.48	0.36	0.38	0.36	0.41	0.61	0.41	6.4	6.4	6.4	5.7	4.1	6.2	27
27	4.5	4.9	4.4	0.48	0.36	0.2	0.25	0.36	0.41	0.33	7	6.6	6.4	6.5	6.3	6.5	67
28	4	5.1	4.9	0.43	0.58	0.41	0.33	0.58	0.61	0.38	7.9	7.8	7.8	7.1	7	6.8	44

29	4.8	4.5	4.4	0.43	0.48	0.43	0.36	0.43	0.38	0.51	7.5	7.6	7.3	6.8	7.2	6.4	56
30	4.4	4.4	4.8	0.25	0.25	0.3	0.3	0.33	0.25	0.28	7	7.3	7.5	6.9	6.6	6.2	50
31	5	5.1	5.2	0.58	0.76	0.51	0.41	0.46	0.38	0.51	7.7	7.7	7	5.9	4.9	6.1	31
32	5.4	5.1	5.2	0.46	0.36	0.41	0.53	0.53	0.46	0.38	7.8	7.6	8	7.1	7.5	7.5	80

Indentation measurements showed considerable variation over the range of conditions studied in the DOE. The data presented here shows that indentations on the thin sheet side ranged from 0.2-mm up to 1.65-mm. There was also considerable scatter within each DOE run. The weld button size data for the 1-2 interface presented here was taken directly from the 1-2 interface tensile-shear tests.

Nugget penetrations into the thin sheet were measured from metallographic specimens. One weld was taken from each trial and used for this sectioning. For each micrograph, the minimum distance from the top sheet external surface and the apparent top sheet thickness were measured. Penetrations were then calculated from the equation:

$$\% Penetration = \frac{t_S - t_R}{t_S} \times 100\% \quad (2)$$

where  $t_S$  and  $t_R$  are the total and residual sheet thicknesses as measured from the micrographs. Penetrations measured in this way are seen to vary from 0% up to 80% throughout this experiment. Micrographs showing extremes in penetration are shown in Figures 1 and 2. Figure 1 is taken from Trial 7, and represents conditions of 0% penetration. From this micrograph it is clear that the weld nugget at best just touches the thin attached sheet, with no effective penetration. Alternately, micrograph taken from Trial 32 (Figure 2) shows a nugget that penetrates nearly to the exterior surface of the thin attached sheet. It is of note in these micrographs that the weld morphology appears to be nearly two superimposed nuggets. This is believed to be an artifact of the dual pulse schedule used for both of the trials shown in Figures 1 and 2.

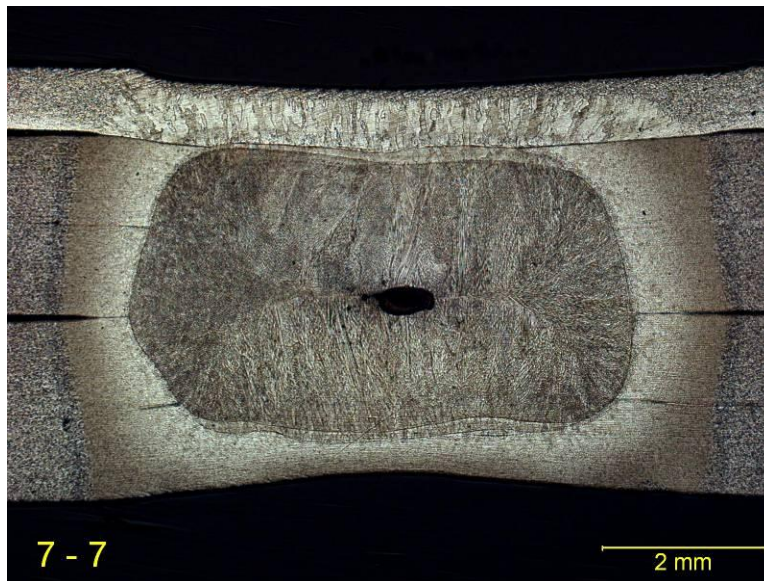


Figure 1: Cross Section of the Weld in Trial 7, Showing 0% Penetration into the Attached Thin Sheet (This weld was made under conditions of a Class 2 electrode on the thin sheet side, a 6.3-mm electrode on the thick sheet side, a 420-ms weld time, two pulses in the main current, a secondary to primary force ratio of 1.5, a primary to total weld time ratio of 0.65, a 2400-N weld force, and a secondary to primary current ratio of 1.4)

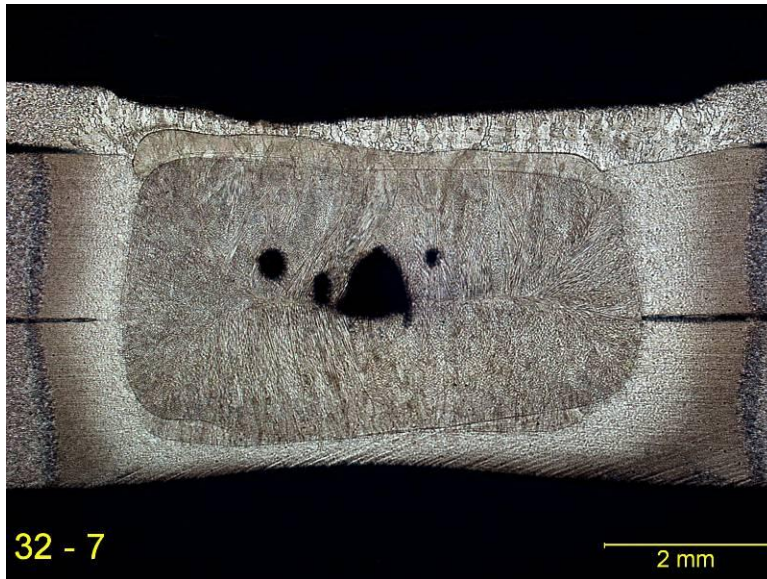


Figure 1: Cross Section of the Weld in Trial 32, Showing 80% Penetration into the Attached Thin Sheet (This weld was made under conditions of a Class 3 electrode on the thin sheet side, a 8-mm electrode on the thick sheet side, a 280-ms weld time, two pulses in the main current, a secondary to primary force ratio of 1.5, a primary to total weld time ratio of 0.4, a 2400-N weld force, and a secondary to primary current ratio of 1.4)

### Statistical Analyses

As described above, all response data sets were evaluated for normality prior to regression curve fitting. This was done by generating a comparative normal dataset based on the calculated means and standard deviations for the test dataset, and correlating this with the actual test data. Where normality could be improved, appropriate transformation functions were used. These transformation functions were derived in an iterative manner, maximizing the correlation of the response data with the comparative normal dataset. All response datasets with the exception of the shear load at the 1-2 interface and thin sheet nugget penetration required normality correction.

Regression correlations of these sets of results range from moderate (transformed button size at the 1-2 interface,  $R^2=56\%$ ) to excellent (penetration,  $R^2=94\%$ ). Generally, the quality of the fit degraded with two aspects of the respective datasets. These included low overall variation in the data from trial to trial, and a high degree of variation within the trial. This is most clearly demonstrated in the case of the transformed button size at the 1-2 interface. Here, the average measured button size from trial to trial varied by less than 3-mm, and replicate results within a trial were seen to achieve similar levels.

### Process Robustness Plots

The regression analyses were then used to prepare process robustness plots for each of the response variables studied. The resulting plots for the eight responses evaluated in this study are provided in Figures 3 to 5. All plots have been anchored at the same baseline set of conditions for the input factors. These conditions have been defined empirically through comparison of the plots for the different response characteristics. Performance was optimized in these plots by maximizing weld nugget penetrations into the thin sheet, button sizes, and joint strengths while minimizing indentations. In addition, allowance was made to provide a set of anchor conditions that are consistent with current industry practice [22]. Specifically, this meant using Class 2

electrodes and a matching (6.3-mm) face diameter on the thick sheet side of the joint. Anchor conditions for these plots then included, as follows:

- Class 2 upper electrode
- 6.4-mm electrode face diameter on the thick sheet side of the joint
- A total weld time of 284 ms
- 40% of the overall weld time in Stage 1
- A single weld pulse for Stage 2
- A 2400-N Stage 1 weld force
- A 50% increase in weld force from Stage 1 into Stage 2
- A 40% increase in weld current from Stage 1 into Stage 2

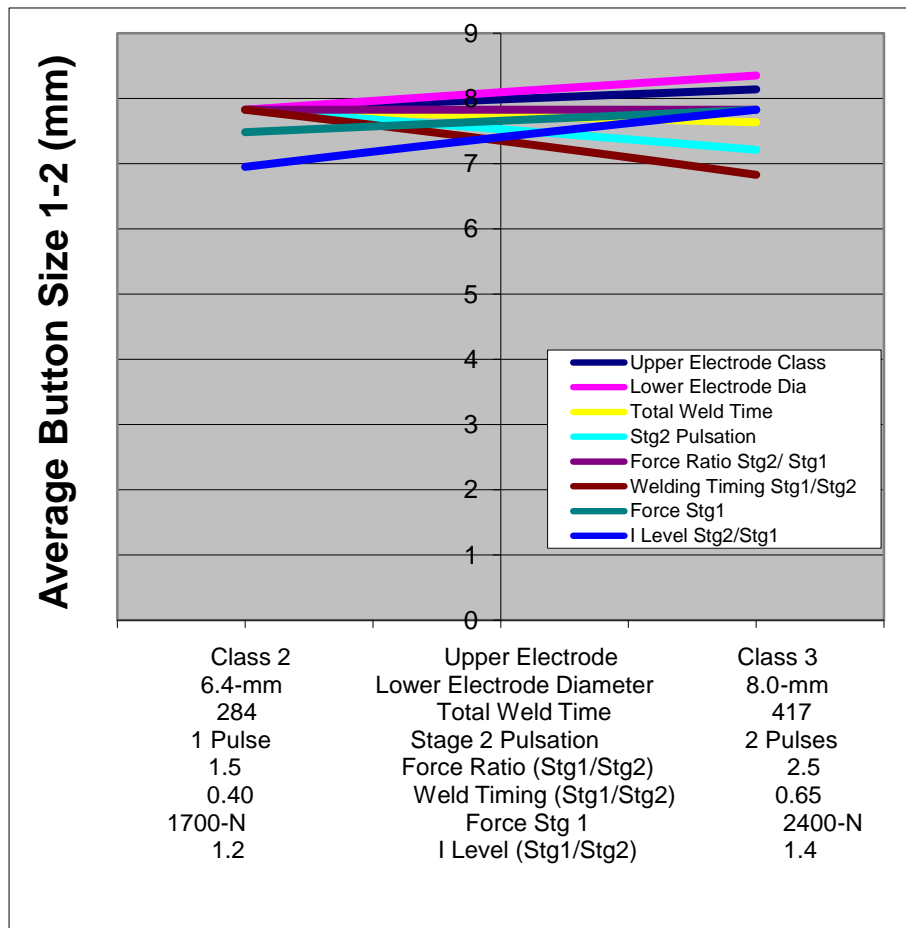


Figure 2: Process Robustness Plot Showing the Effects of the DOE Variables on the Average Button Size at the Thin/Thick (1-2) Interface (The plot is anchored at base conditions of a Class 2 upper electrode, a 6.4-mm electrode face diameter on the thick sheet side of the joint, 284-ms total weld time, with 40% of the overall weld time in Stage 1, a single weld current pulse for Stage 2, a 2400-N Stage 1 weld force, a 50% increase in weld force from Stage 1 into Stage 2, and a 40% increase in weld current from Stage 1 into Stage 2)

The resulting plot for the measured button size at the 1-2 interface is provided in Figure 3. At anchor conditions, the plot suggests a button size of almost 8-mm can be achieved. This is in excess of the generally accepted  $6\sqrt{t}$  criteria incorporated in many recommended practices and specifications [4, 5, 6, 22]. Of note, none of the plotted variations from these anchor conditions resulted in predicted button sizes below 6.8-mm or above 8.4-mm. The process robustness plot for the degree of electrode indentation at the thin sheet surface is provided in Figure 4. Here, the anchor conditions used resulted in nominally 0.45-mm of indentation into the thin attached sheet. This corresponds to roughly 45% indentation of the sheet on that side of the joint. Further, the robustness plot suggests that indentation is sensitive to a range of the DOE factors. Specifically, greater indentations could be driven by larger thick sheet side electrode diameters (up to 0.85-mm), higher forge/weld force ratios (up to 0.75-mm) as well as a Class 3 electrode on the thin sheet side (up to 0.65-mm). Conversely, indentations could be reduced by use of relatively longer Stage 1 currents (down to 0.33-mm), pulsation during the Stage 2 current (0.36-mm), a lower relative Stage 2 current (0.35-mm), and a lower welding force (0.38-mm).

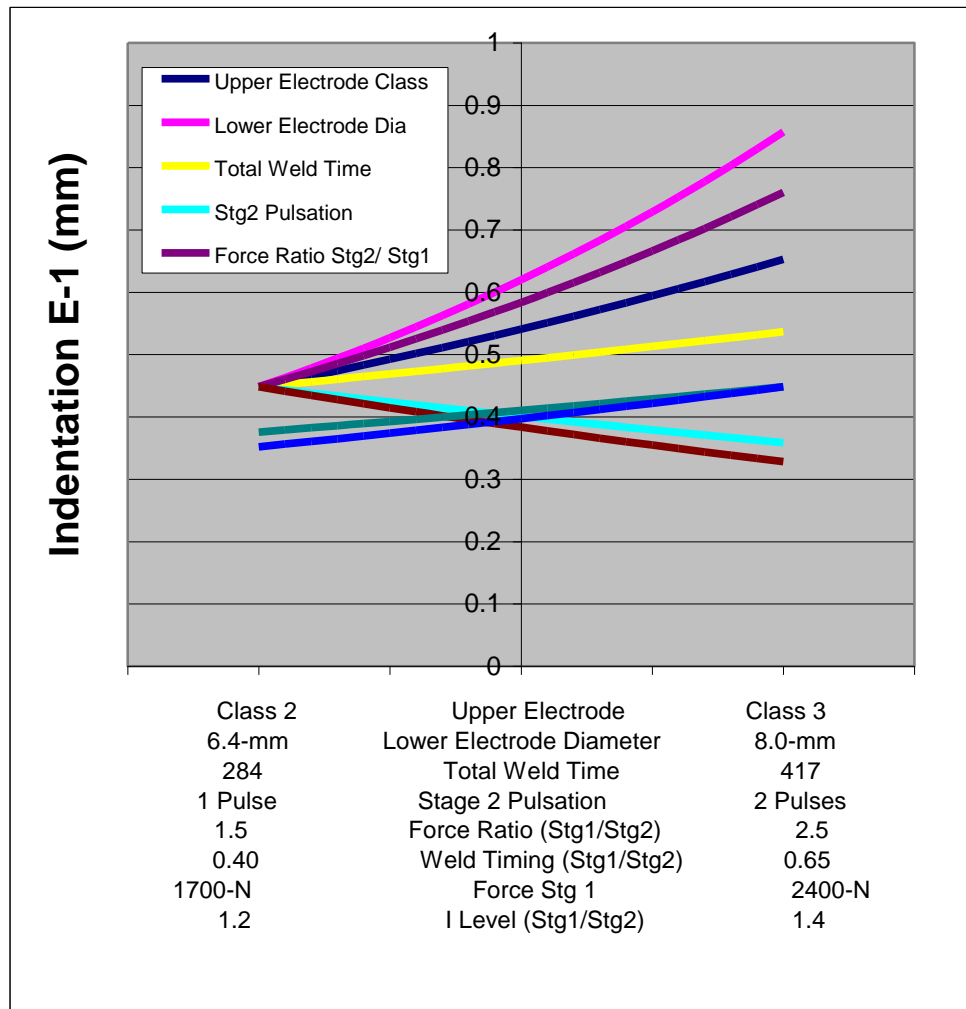


Figure 3: Process Robustness Plot Showing the Effects of the DOE Variables on the Measured Indentation at the Thin Sheet (E-1) Surface (The plot is anchored at base conditions of a Class 2 upper electrode, a 6.4-mm electrode face diameter on the thick sheet side of the joint, 284-ms total weld time, with 40% of the overall weld time in Stage 1, a single weld current pulse for Stage 2, a 2400-N Stage 1 weld force, a 50% increase in weld force from Stage 1 into Stage 2, and a 40% increase in weld current from Stage 1 into Stage 2)

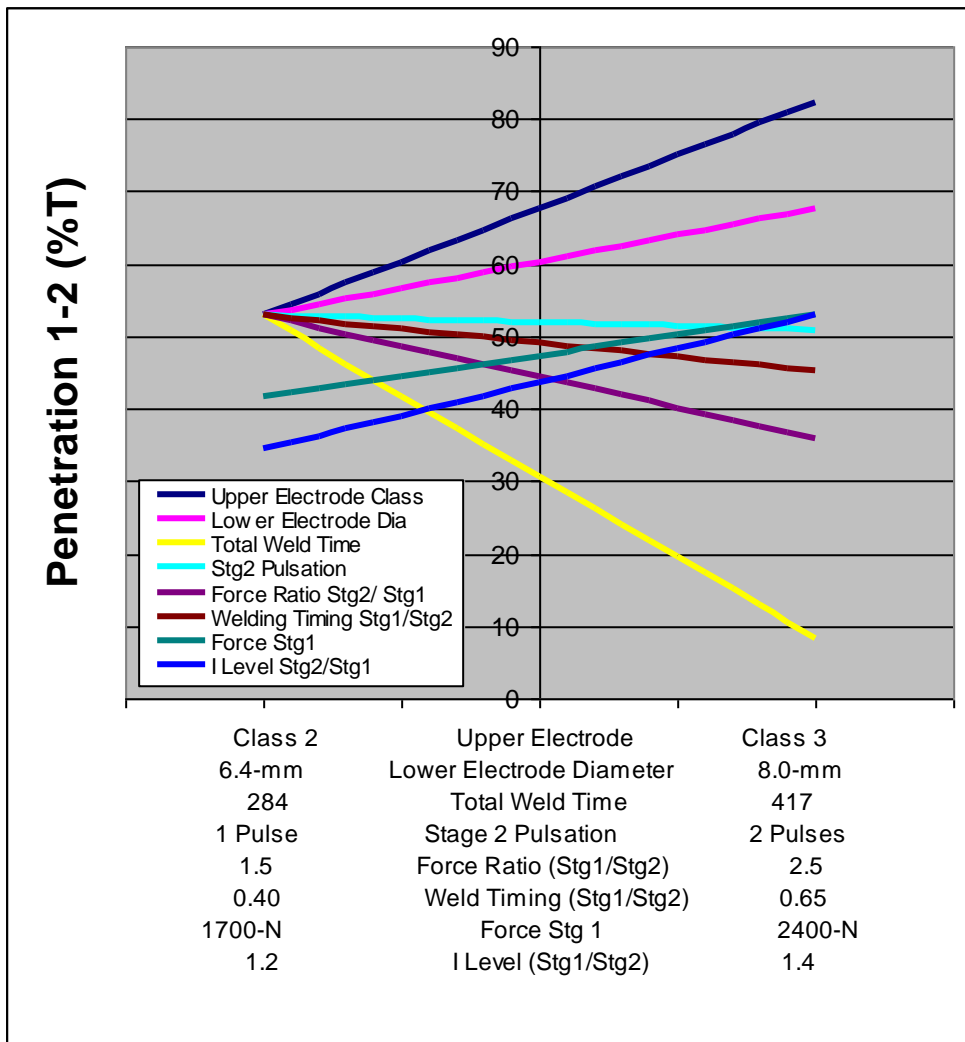


Figure 4: Process Robustness Plot Showing the Effects of the DOE Variables on the Nugget Penetration into the Thin Attached Sheet (1-2 Interface) (The plot is anchored at base conditions of a Class 2 upper electrode, a 6.4-mm electrode face diameter on the thick sheet side of the joint, 284-ms total weld time, with 40% of the overall weld time in Stage 1, a single weld current pulse for Stage 2, a 2400-N Stage 1 weld force, a 50% increase in weld force from Stage 1 into Stage 2, and a 40% increase in weld current from Stage 1 into Stage 2)

Finally, the process robustness plot for the degree of penetration into the outside thin sheet is presented in Figure 5. At anchor conditions, this penetration was estimated at roughly 0.53-mm. This penetration, however, is affected by a number of the DOE factors. Particularly, variations in the electrode configurations themselves appear most affective at increasing penetrations. For example, increasing the thin sheet side electrode to Class 3 copper increases penetrations to over 0.8-mm, while use of an 8-mm electrode on the thick sheet side electrode results in estimated penetrations of nearly 0.7-mm. Penetration is most adversely affected by lengthening the weld time. Here, increasing the weld time to 417 ms reduces the estimated penetrations to less than 0.1-mm. Higher relative Stage 2 weld currents, lower weld forces, shorter relative Stage 1 welding times, and the use of pulsation were all detrimental to nugget penetrations. The effect in each case was less than 0.15-mm.

## Discussion

It is of note in this study that overall best penetrations into the thin attached sheet of this stack-up were achieved using variations in electrodes. This included using differentially sized electrodes (larger electrode on the thick sheet side of the joint), as well as different thermal conductivity electrodes. The results here generally confirm the recommendations made in both the Resistance Welding [4] and Welding [5] Handbooks. That is, changing the heat extraction of capabilities of the electrodes on either side of the joint can effectively move the heat center of the stack-up.

### **Manufacturing Considerations of the Selection of Baseline Conditions in this Study**

The discussion above underscores the dominance of electrode variations in achieving attachment of thin-sheet outside elements in complex stack-ups. However, as mentioned previously in this report, the application of different electrodes to the two sides of such stack-ups in actual automotive manufacture can be problematic at best. The use of different electrodes has direct cost implications. Specifically, both electrode types must be inventoried, adding cost to the process. In addition, there are concerns that in modern automotive manufacturing a single gun may be used to make spot welds on a range of stack-ups as part of a single operation. Mandating dissimilar electrode combinations for specific complex stack-up joints carries the suggestion of dedicated welding guns for specific joints. The use of such dedicated guns inherently increases capital requirements and reduces flexibility. Both directly affect manufacturing costs in a detrimental way. The final concern associated with dissimilar welding electrodes is related to maintenance. In high volume manufacturing environments, there is concern about confusing electrodes during replacements where large numbers of caps may be replaced simultaneously. As might be anticipated, reversal of caps on a complex stack-up would tend to move the heat center away from the desired location, with catastrophic results in a manufacturing environment.

For these reasons, use of dissimilar electrodes cannot be considered a solution to attaching thin outer sheets in a complex stack-up. As a result, the use of similar-sized, similar material electrodes were selected in the process robustness studies conducted here as part of the baseline conditions. Definition of a best welding practice for servo-guns must then be focused on optimizing weld times, as well as weld/forge force and current ratios.

### **Best Practices for Attachment of Thin Sheets in Complex Stack-Ups**

Optimization of the remaining DOE variables in this study to achieve best penetrations on the thin sheet side of the joint suggested the use of the following conditions; short overall weld times, moderate forge force-to-weld force ratios, and high forge current-to-weld current ratios. Of these, weld time effects were dominant. The use of shorter weld times to achieve improved heat balances is not unknown. Shorter weld times (and higher currents) are known to react more aggressively with available contact resistances, preferentially heating the various interfaces in the stack-up. As a result, there is tendency to more readily heat the thin/thick interface, increasing both the degree of subsequent nugget penetration and likelihood of attachment. Of interest, higher forces and moderate forge/weld force ratios both improved penetrations. In the former case, this is believed to be related to the ability to grow larger weld nuggets before expulsion (thin/thick sheet button sizes also increased).

The increases in penetration related to the reduced relative forge forces is believed to be associated with indentation effects. It is observed that at higher relative forge forces, indentations also increased. This increase

in indentation has the effect of suddenly changing the geometry of the weld relative to the temperature field. As this occurs, there is a re-distribution of heat in accordance with the new geometry. This re-distribution appears to reduce the fraction of the remaining thin sheet contained within the nugget, effectively reducing effective penetrations on this side of the joint.

Finally, as noted above, higher forge/weld current ratios appeared to have a beneficial influence on nugget penetration. This suggests that there may be some secondary growth of the weld nugget (during forging) improving the resulting penetrations.

As described above, under baseline practice conditions as defined in this DOE, penetrations of over 50% (0.5-mm) could be obtained into the thin sheet. Of note, once these baseline practices are defined, that joint strengths are relatively insensitive to any of the process variations studied (not including electrode variations). The major tradeoff appears to be between penetrations and indentations. Under the baseline conditions, electrode indentations of roughly 0.45-mm (45% of the thin sheet thickness) are observed. This may or may not be considered excessive based on some automotive specifications. Of note, the DOE results do suggest some potential tradeoffs between nugget penetration and indentation. Specifically, increased relative weld time as well as reduced forces each individually offer reductions in electrode indentation of roughly 0.1-mm while maintaining nugget penetrations greater than 0.4-mm (40%). Most beneficial tradeoffs between these two characteristics will undoubtedly be defined by the individual application.

## **Conclusions**

In this program, the resistance spot weldability of complex stack-ups has been investigated with respect to the capabilities of new-generation MFDC electric servo-guns. These systems include capabilities for varying both current and force profiles during the welding cycle. This investigation was conducted on a specific complex stack-up, incorporating a 1- to 2-mm arrangement. Weldability was assessed using DOE techniques. Factors studied in this experiment included the use of differential electrode materials and sizes, primary welding forces, total welding times, time fractions of primary current flows, numbers of pulses in the secondary current flow, ratios of forge to welding currents, and ratios of forge to welding forces. Response variables in this DOE included button sizes at both the thin/thick and thick/thick interface, indentations at the thin sheet and thick sheet sides of the joint, and nugget penetration into the thin sheet. The DOE was then used to produce robustness plots for each response variable. Comparison of these robustness plots allowed definition of some baseline processing conditions for creating these joints. Individual plots then allowed interpretation of performance variations associated with each variable studied in the DOE. It was found that nugget penetration results were dominated by electrode considerations. This is consistent with previous work on complex stack-ups. However, it was also noted that such side to side electrode variations are not compatible with current manufacturing practices. For similar electrode configurations, best penetrations into the thin attached sheet were accomplished through short overall weld times, short heat times before forging, higher weld forces, a 50% increase in the force on forging, and a 40% increase in current during the forge stage. This resulted in nugget penetrations of roughly 50% into the thin sheet, and indentations (on the thin sheet side) of less than 0.5-mm.

## References

1. Dinda, S. and Diaz, R., "The Partnership for a New Generation of Vehicles (PNGV) and its Impact on Body Engineering", *Proc. IBEC 95, Advanced Technologies and Processes*, pp. 5-8, IBEC Ltd (1995).
2. Crooks, M. J. and Miner, R. E., "The Ultralight Steel Auto Body Program completes Phase I", *Journal of Metals*, 48(7):13-15 (1996).
3. Bleck, W., "Cold Rolled, High-Strength Sheet Steels for Auto Applications", *Journal of Metals* 48(7):26-30 (1996).
4. *Resistance Welding Manual, Fourth Ed.*, Resistance Welder Manufacturers Association, Miami, FL (2003).
5. *Welding Handbook*, 9<sup>th</sup> Ed., Vol. 3, Welding Processes, Part 2, American Welding Society, Miami, FL, pp. 1-48 (2007).
6. "A/SP Starting Resistance Spot Weld Schedules for AHSS", Auto-Steel Partnership, Detroit, MI (2008).
7. Lu, F., Karagoulis, M. J., and Dong, P., "The Influence of Different Sheet Combinations on Nugget Development during Resistance Spot Welding of Thick Stack-Ups", *Sheet Metal Welding Conference IX*, Detroit AWS Section, Detroit, MI. Paper 1-4 (2000).
8. Fong, M., Tsang, A., and Ananthanarayanan, A., "Development of the Law of Thermal Similarity (LOTS) for Low-Indentation Cosmetic Resistance Welds", *Sheet Metal Welding Conference IX*, Detroit AWS Section, Detroit, MI. Paper 5-6 (2000).
9. Agashe, S. and Zhang, H., "Selection of Schedules Based on Heat Balance in Resistance Spot Welding", *Sheet Metal Welding Conference X*, Detroit AWS Section, Detroit, MI. Paper 1-2 (2002).
10. Anderson, C., Wiermaa, C., and Morel, M. K., "Developments in Resistance Spot Welding", *Practical Welding Today*, 4(6): 38-40 (2000).
11. Slavic, S. A., "Using Servo-Guns for Automated Resistance Welding", *Welding Journal*, 29-33 (1999).
12. Barthelemy, P., "Servo Weld Gun – Present and Future", *Sheet Metal Welding Conference XI*, Detroit AWS Section, Detroit, MI. Paper 3-7 (2004).
13. Grimes, P., "Advantages of using Servo Force Control when Resistance Welding Aluminum Sheet Metal", *Sheet Metal Welding Conference XII*, Detroit AWS Section, Detroit, MI. Paper 6-2 (2006).
14. Lehman, L. R. and Gould, J. E., "A Study of Resistance Spot Welding Manufacturability Using Design-of-Experiments," *International Body Engineers Council (IBEC) 94 Proceedings, Advanced Technologies and Processes*, pp. 154-163, Warren, MI, IBEC Ltd. (1994).

15. Lehman, L. R. and Gould, J. E., "A Design-of-Experiments Evaluation of Resistance Spot Welding Manufacturability - Part 2: Multiple Factor Effects," *IBEC 95 Proceedings, Advanced Technologies and Processes*, pp. 88-99, Warren, MI, IBEC Ltd. (1995).
16. Lehman, L. R. and Gould, J. E., "A Design-of-Experiments Evaluation of Resistance Spot Welding Manufacturability - Part 3: Optimization and Process Robustness Studies," *IBEC 96 Proceedings, Advance Technologies and Processes*, Warren, MI, IBEC Ltd. (1996).
17. Galiher, D., Tower Automotive, private communication (2007).
18. Bohr, J., General Motors Corporation, private communication (2007).
19. Pakalnins, N., Chrysler LLC, private communication (2007).
20. Wexler, A., Ford Motor Company, private communication (2007).
21. Schnipke, K., Honda of America, private communication (2007).
22. "Recommended Practices for Test Methods for Evaluating the Resistance Spot Welding Behavior of Automotive Sheet Steel Materials", AWS/SAE D8.9M:2002 (2002).
23. Gould, J. E., "Modeling Primary Dendrite Arm Spacing in Resistance Spot Welds, Part 2 - Experimental Studies", *Welding Journal Research Supplement*, 73(5):91s-100s (1994).

### **Acknowledgements**

EWI acknowledges the contribution of the State of Ohio, Department of Development and Thomas Edison Program, which provided funding in support of Edison Technology and Industry Center Services.